



A ratiometric fluorescent probe based on the pi-stacked graphene oxide and cyanine dye for sensitive detection of bisulfite

Huan Yu^{a,b,d,1}, Libo Du^{c,1}, Lingmei Guan^c, Kui Zhang^b, Yingyun Li^b, Houjuan Zhu^b, Mingtai Sun^{b,**}, Suhua Wang^{a,b,d,*}

^a School of Environmental and Chemical Engineering, North China Electric Power University, Beijing 102206, People's Republic of China

^b Institute of Intelligent Machines, Chinese Academy of Sciences, Hefei, Anhui 230031, People's Republic of China

^c State Key Laboratory for Structural Chemistry of Unstable and Stable Species, Center for Molecular Sciences, Institute of Chemistry, Chinese Academy of Sciences, Beijing 100190, People's Republic of China

^d Department of Materials Science and Engineering, University of Science and Technology of China, Hefei, Anhui 230026, People's Republic of China

ARTICLE INFO

Article history:

Received 13 December 2016

Received in revised form 15 March 2017

Accepted 18 March 2017

Available online 20 March 2017

Keywords:

Fluorescent probe

Ratiometric

Sulfur dioxide

Ratio imaging

Nanocomposite

ABSTRACT

The sensitive and selective analytical methods for real-time monitoring of sulfur dioxide and its derivatives are significant for human health, pollution-control and food safety. Herein, we report a new nanocomposite (Hex-FGO-DPS) consisting of cyanine dye and fluorescent graphene oxide with unique reactive properties for ratiometric fluorescent detection of bisulfite. The ratiometric fluorescence of Hex-FGO-DPS in aqueous solution can be sensitively, selectively and efficiently tuned by bisulfite through a specific nucleophilic addition reaction. In the presence of bisulfite, the ratiometric fluorescence intensity of Hex-FGO-DPS ($F_{470\text{nm}}/F_{580\text{nm}}$) changes up to 25 folds, accompanied by a distinct color change from yellow to blue which can be visually identified. The detection limit was measured to be 0.44 μM . The probe can be further applied for sensing intracellular bisulfite through the ratiometric fluorescence imaging analysis in living cells. In addition, the probe Hex-FGO-DPS also can be used for selective determination of gaseous sulfur dioxide in atmosphere and aqueous solution. The simple, sensitive and effective strategy reported here could facilitate the development of portable and reliable sensor for visual identification applications.

© 2017 Elsevier B.V. All rights reserved.

1. Introduction

Sulfur dioxide is a sulfur-containing molecule and air pollutant, which is derived from coal-fired industry and paroxysmal eruption of volcano and also can be produced endogenously from oxidization of sulfur-containing amino acids [1–3]. Sulfur dioxide in the atmosphere and in vivo is readily hydrated to bisulfite and sulfite, which can cause a variety of respiratory diseases, cardiovascular diseases and even worse is lung cancer [4–6]. Due to the intrinsic antimicrobial and antioxidant properties, sulfur dioxide and its derivatives have been commonly used as additives in food, wine and drugs to prevent oxidation. Over-exposure to sulfur dioxide inhalation or intake of excess bisulfite and sulfite are serious to human health.

Therefore, the contents of bisulfite and sulfite as food additives have been strictly restricted by food safety regulations. Therefore, new sensitive analytical methods for sulfur dioxide and its derivatives have significance for food and pharmacy quality control, environmental protection, and biological study in vivo. Some conventional methods have been reported for the detection of sulfur dioxide and its derivatives by using different signal recognition strategies, such as chromatograph [7–9], electrochemistry [10,11], capillary electrophoresis [12–14] and absorption spectrophotometry. Compared with these methods, fluorometry based methods show high sensitivity and optical signal output, which have the capability for visualization. A few fluorescent probes for sulfur dioxide and its derivatives have been reported based on nucleophilic addition [15–23], deprotection of levulinate group [24,25], complexation of azo group [26,27] and sulfitation of aldehydes [28–31]. Herein, we synthesize a ratiometric fluorescent probe by integrating graphene oxide and cyanine dye and demonstrate the application for sensitive detection and visualization of sulfur dioxide and its derivatives in vivo.

* Corresponding author at: School of Environmental and Chemical Engineering, North China Electric Power University, Beijing 102206, People's Republic of China.

** Corresponding author at: Institute of Intelligent Machines, Chinese Academy of Sciences, Hefei, Anhui 230031, People's Republic of China.

E-mail addresses: mtsunsun@iim.ac.cn (M. Sun), shwang@iim.ac.cn (S. Wang).

¹ These authors contributed equally to this work.

Graphene oxide (GO) is a two-dimensional nanomaterial derived from graphite and has been extensively explored for applications in biomedicine, catalysis, electronics, and so forth. Graphene oxide has rarely been investigated in sensing applications because of its relatively low fluorescence quantum yield (QY). Blue fluorescent GO can be produced by modifying the superficial epoxy and carboxylic groups with alkylamines, restrain the non-radiative recombination of localized electron-hole (e-h) pairs [32–37]. The large conjugated system made GO as a nanocarrier such that it may engage fluorophores, nucleic acid, and peptide through a full complement of noncovalent interactions. The nanocarrier function of GO can readily interact with aryl compounds through π - π stacking interaction [38–40]. The architecture interaction of graphene oxide and aryl compound can be devised for new analytical approaches.

Herein, we designed a new ratiometric fluorescent sensor for gaseous sulfur dioxide, bisulfite and sulfite in atmosphere and living cells. We first synthesized a cyanine derivative (DPS) containing an alkene unit as bisulfite recognition site, and then assemble the cyanine derivative on the surface of hexamethylenediamine modified fluorescent GO (Hex-FGO) through electrostatic interaction. Based on cyanine dye, a few of redox-responsive fluorescent probes for ROS have been designed [41–43]. The obtained ratiometric fluorescent probe (Hex-FGO-DPS) has a unique reactivity to bisulfite and produced distinctive fluorescence color variation from yellow to blue. The molecular structure of DPS and its complex with Hex-FGO is displayed in Scheme 1. With the assistance of Hex-FGO, the nanocomposite Hex-FGO-DPS exhibits a sensitive ratiometric response toward bisulfite than free chemodosimeter DPS. Such material has also been successfully applied for the ratiometric fluorescence imaging of bisulfite in living cells.

2. Materials and methods

2.1. Materials

The chemicals included reactants, metal ions and inorganic anions were obtained from the commercial sources (Sigma Aldrich or Aladdin) and used directly without further purification unless specified. All kinds of organic solvent were purchased from Sinopharm Chemical reagent co., Ltd (Shanghai) and purified and dried by a standard method for purification and drying. Aqueous solutions were all prepared using ultrapure water (18.2 M Ω cm) from a Millipore water purification system and all glassware were cleaned with ultrapure water, and then dried before use. Standard SO₂ gas was purchased from Nanjing Special Gas Factory Co. Ltd. Standard NO and NO₂ gas were purchased from Changzhou Jinghua Industrial Gases Co., Ltd.

2.2. Instrumentation and methods

Fluorescence measurement was recorded on a Perkin-Elmer LS-55 luminescence spectrometer (Liantriant, UK) equipped with a plotter unit and a quartz cell (1 cm \times 1 cm). UV-vis absorption was recorded at room temperature on a Shimadzu UV-2550 spectrometer. Photographs were taken with a canon 350D digital camera. pH values are measured by PHS-3C pH meter. ¹H NMR spectra were measured using a Varian Mercury-400 NMR spectrometer, and Mass spectra were performed on a Thermo Proteome X-LTQ MS mass spectrometer in ES positive or negative mode. Silica gel-60 (230–400 mesh) was used as the solid phases for column chromatography. Thin-layer chromatography (TLC) was performed by using Merck F254 silica gel-60 plates. TLC plates were viewed with UV light within the wavelength of 365 nm. Confocal images were scanned by Laser Confocal Microscopy (OBSERVER Z1, ZEISS) and a

60 \times oil-immersion objective lens. MCF-7 (Michigan Cancer Foundation –7) was purchased from American Type Culture Collection (ATCC). They were cultured in the DMEM with 10% fetal bovine serum (FBS) at 37 °C in humidity incubator containing 5% CO₂.

2.3. Synthesis of 2, 3, 3-Trimethyl-1-(3-sulfonatepropyl)-3H indolium

2,3,3-trimethylindolenine (2 g, 12.56 mmol) was first added to a solution of 1,3-propane sultone (422 mg, 3.45 mmol) in 1, 2-dichlorobenzene (3 mL). The reaction mixture was stirred at 120 °C for 18 h. The purple precipitate (804 mg, 91%) was collected by filtration and washed with cold diethyl ether and dried in vacuo.

2.4. Synthesis of (E)-3-(2-(2-(6-methoxynaphthalen-2-yl)vinyl)-3,3-dimethyl-3H-indolium-1-yl)propane-1-sulfonate (DPS)

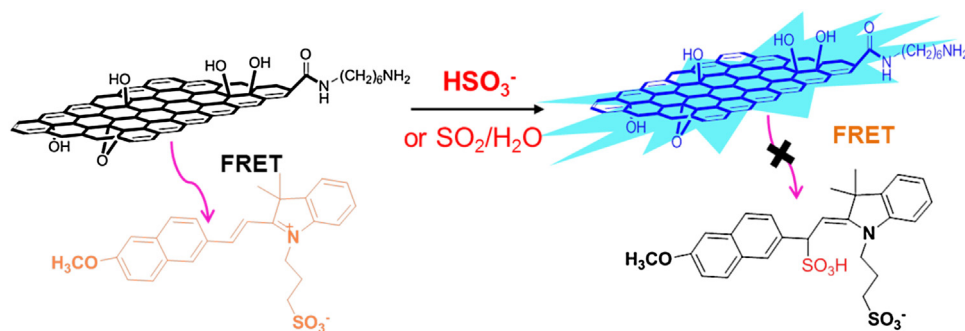
A mixture of 6-methyl-2-naphthaldehyde (0.06 mmol) and indolium derivative (0.07 mmol) was dissolved in 15 mL ethanol. Then several drips of piperidine was added in the reaction mixture and stirred for 4 h at 80 °C under a nitrogen atmosphere. After reaction, the mixture was concentrated by evaporation under reduced pressure. The crude product was purified on silica gel chromatography eluted with dichloromethane/methanol (10:1 v/v) to give the desired product as an orange solid. Yield (60.2%). HR-MS: *m/z* calcd for C₂₆H₂₈NO₄S [M+H]⁺, 450.1739; found 450.1735. ¹H NMR (400 MHz, DMSO) δ 8.79 (s, 1H), 8.62 (d, *J* = 15.9 Hz, 1H), 8.42 (d, *J* = 8.7 Hz, 1H), 8.12–7.94 (m, 4H), 7.89 (d, *J* = 6.7 Hz, 1H), 7.63 (s, 2H), 7.48 (s, 1H), 7.30 (d, *J* = 9.1 Hz, 1H), 4.90 (s, 2H), 3.95 (s, 3H), 2.72 (s, 2H), 2.23 (s, 2H), 1.85 (s, 6H). ¹³C NMR (101 MHz, DMSO) δ 182.12, 160.46, 154.99, 144.27, 141.32, 137.64, 135.11, 131.71, 130.71, 129.55, 128.48, 128.21, 127.63, 125.99, 124.87, 123.52, 121.82, 120.22, 119.28, 115.54, 112.25, 107.15, 99.37, 56.05, 52.56, 49.81, 48.98, 47.71, 26.20, 20.62.

2.5. Synthesis of hexanediamine modified fluorescence graphene oxide (Hex-FGO)

For the preparation of fluorescent graphene oxide, graphene oxide was used as starting material prepared by a classical Hummers method. Then hexanediamine modified fluorescence graphene oxide was synthesized by a reported procedure (Zhu et al., 2014). A solution of 30 mg graphene oxide in 10 mL DMF was added in 30 mL SOCl₂ and then refluxed at 80 °C for 24 h. The underlying precipitate was collected and washed with anhydrous THF twice and then centrifugation at 10000 rpm for 10 min. Then, the prepared GO acyl chloride was dispersed in anhydrous tetrahydrofuran and further added hexanediamine for stirring at 80 °C for 48 h. After the reaction, final pale yellow supernatant was collected and then dried by vacuum drier. 10 mg of the obtained Hex-FGO was re-dispersed in ethanol (20 mL) to form light yellow suspension (0.5 mg/ml) for further use.

2.6. In vitro detection of bisulfite by the nanocomposite

A mixture solution of DPS and Hex-GO was obtained by the addition of 1.5 mg of Hex-GO to 3 mL of DPS (5 mM) ethanol solution to get a nanocomposite Hex-FGO-DPS. Generally, 2 μ L of stock solution of Hex-FGO-DPS (5 mM) in ethanol was diluted in 2.0 mL of 50 mM phosphate buffer (pH 7.0) to obtain a final concentration of 5 μ M. The concentration of nanocomposite was defined as the concentration of DPS in the nanocomposite ethanol solution. GSH, Cys, F⁻, I⁻, NO₂⁻, AcO⁻, HPO₄⁻, S₂O₃⁻, S₂O₈⁻, SCN⁻ were freshly prepared with a stock solution concentration of 20 mM.



Scheme 1. Schematic illustration of the nanocomposite probe's structure and recognition principle for bisulfide.

Sulfide solution was prepared with a stock solution concentration of 10 mM. All fluorescence spectra were recorded in the range from 400 to 730 nm using a 370 nm excitation wavelength and a 500 nm/min scan rate.

2.7. Confocal fluorescence imaging

For cell imaging of HSO_3^- , MCF-7 cells were prepared in confocal plates (1×10^5 cells per well) and treated with 5% CO_2 at 37°C in a humidity incubator for 24 h. For the control experiment, four confocal plates of MCF-7 cells were incubated with 10 μM of Hex-FGO-DPS at 37°C for 4 h in DMEM medium supplemented with 10% FBS at 37°C and 5% CO_2 , then washed with 1 mL of phosphate buffer saline (pH 7.4) twice. For the measurement process, different concentration of bisulfite were introduced to three of the plates with final concentration of 25 μM , 50 μM and 75 μM and incubated for another 0.5 h. The cell image were collected under excitation at 405 nm from the blue channel (460–480 nm) and the yellow channel (560–580 nm) using laser confocal microscopy (OBSERVER Z1, ZEISS) and a $60\times$ oil-immersion objective lens.

2.8. The process for gas measurement

Nitric oxide (NO) and nitrogen dioxide (NO_2) was prepared by diluting the pure gas to target concentrations. CO gas was prepared from the reaction of HCOOH with concentrated H_2SO_4 . H_2S gas was prepared from the reaction between Na_2S and 5 M diluted H_2SO_4 . NH_3 gas was prepared from the reaction of NH_4Cl with $\text{Ca}(\text{OH})_2$. O_3 gas was prepared from the ozonizer. Each prepared gas sample (10^3 ppm, NO was diluted in nitrogen gas) was bubbled into a probe solution, followed by collecting the spectra and the fluorescence photos. The concentration of SO_2 gas was measured by dissolving SO_2 gas in ethanol and determined the concentration by measuring the UV absorbance at 277 nm ($\epsilon = 365 \text{ M}^{-1} \text{ cm}^{-1}$) using the Beer-Lambert law.

3. Results and discussion

In the design strategy, unsaturated double bond was chosen as the recognition site towards bisulfite through a specific nucleophilic addition. The recognition site was easily produced through a one-step reaction by using 6-methoxy-2-naphthaldehyde and 3-(2,3,3-trimethyl-3H-indolium-1-yl)propane-1-sulfonate in ethanol (Fig. S1). The introducing of sulfonate unit improved the water solubility. The chemical structure of DPS was confirmed by ESI-MS, ^1H NMR and ^{13}C NMR (Figs. S2–S4). The DPS has maximum excitation wavelength and maximum emission wavelength at 455 and 580 nm, respectively (Fig. S5). DPS displays an absorption maxima at nearly 455 nm and its solution is yellow (Fig. S6). In addition, the probe was not sensitive with the variation of pH value from 4 to 10 (Fig. S7). The reaction between bisulfite and α,β -unsaturated

ketone via Michael addition destroys the π -conjugation of DPS, which result in significant decrease in the absorption and emission intensity. The maximum absorbance at 455 nm decreased obviously accompanied with the disappearance of yellow color. The variation of fluorescence spectra further confirmed the structural transformation due to bisulfite. Clearly, DPS initially emits orange-yellow fluorescence upon excitation at 450 nm, when the amount of bisulfite increased, the orange-yellow fluorescence quenched greatly (Fig. S8).

In order to investigate the reaction mechanism of DPS for HSO_3^- , the electrospray ionization mass spectrometric (ESI-MS) spectra of DPS were systematically performed before and after adding HSO_3^- . The ESI-MS spectrum of DPS shows a dominating peak at $m/z = 450.18 (\text{M}+\text{H})^+$, which is consistent with its molecular value (Fig. S9). However, a new line at $m/z = 530.04 (\text{M})$ appears after reaction with bisulfite. It can be assigned to the addition product because the value is close to the molecular weight of the product. In addition, the sensing mechanism of DPS for bisulfite was also carefully examined by ^1H NMR spectral changes of the probe after addition of HSO_3^- (Fig. S10). Clearly, the proton signal at δ 1.79 (H_c) of the two methyl groups CH_3 shifts forward and splits into two signals (H_c' , at δ 1.45 and 1.57) after reaction with HSO_3^- . The

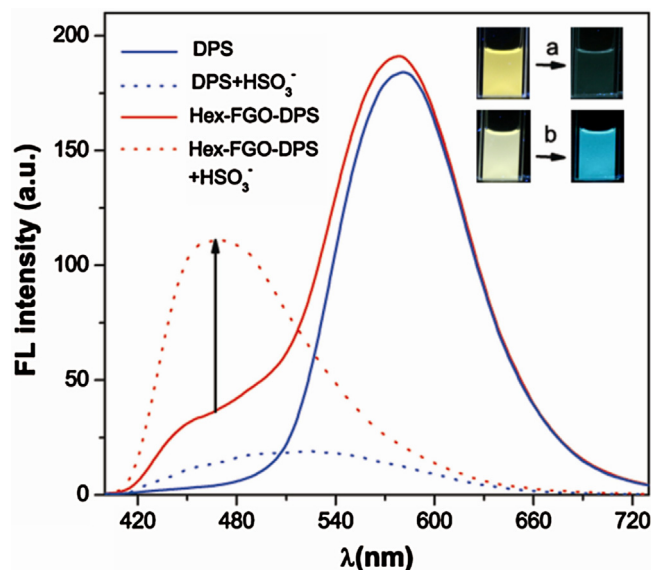


Fig. 1. Blue line: Fluorescence spectra of 5 μM DPS in PBS 7.0 before and after adding 35 μM HSO_3^- . Red line: Fluorescence emission spectra of 5 μM Hex-FGO-DPS before and after adding 35 μM HSO_3^- . The fluorescence spectra were recorded with excitation at 370 nm. The inset photos show the corresponding fluorescence colors variation of DPS (a) and Hex-FGO-DPS (b) before and after adding HSO_3^- under a 365 nm UV lamp, respectively. (For interpretation of the references to colour in this figure legend, the reader is referred to the web version of this article.)

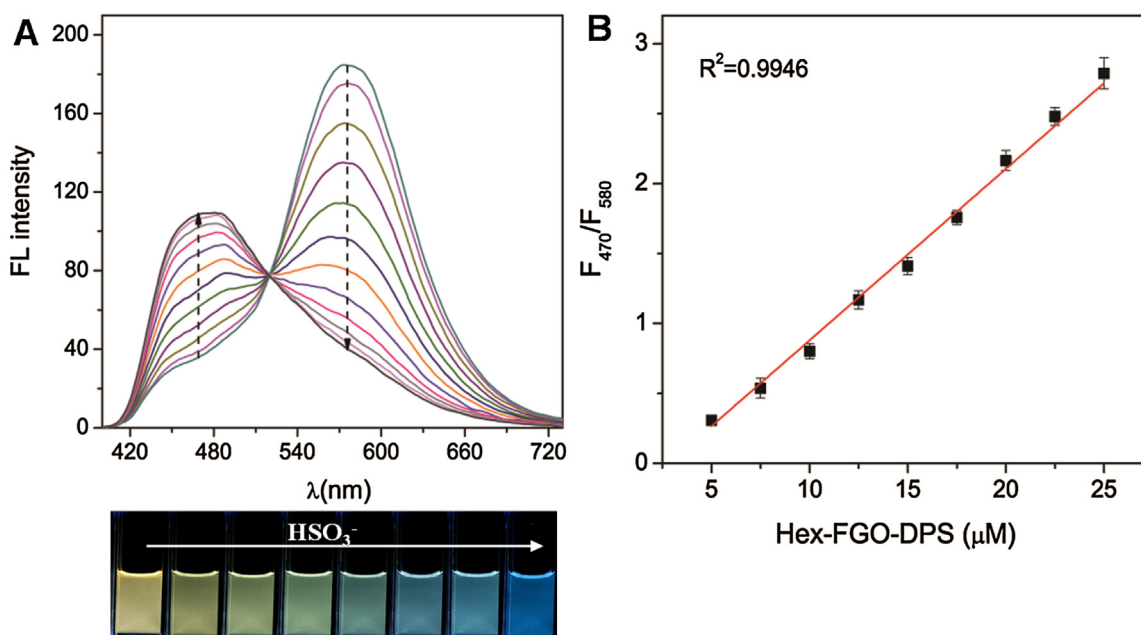


Fig. 2. (A) Ratiometric fluorescence spectra of Hex-FGO-DPS (5 μM) upon the addition of HSO_3^- (5–25 μM). The below graph represents the fluorescence image of Hex-FGO-DPS solution upon the addition of different amounts of HSO_3^- under UV lamp. (B) Plot of ratiometric fluorescence efficiency of Hex-FGO-DPS as a function of HSO_3^- concentration in the range from 5 to 25 μM . F_{470} and F_{580} were the fluorescence intensity of Hex-FGO-DPS at the wavelength of 470 nm and 580 nm, respectively. The fluorescence spectra were recorded with excitation at 370 nm.

proton signals (H_a , at δ 7.42, and H_b , at δ 7.26), which are assigned to the double bond of DPS, also shift to δ 5.00 (H_b') and δ 4.62 (H_a'), respectively. The proton signals (H_d , at δ 4.82), which are assigned to CH_2SO_3^- group, shift to δ 3.65 (H_d'). Moreover, a new signal appeared at δ 9.96 (H_e'), which can be explained by the nucleophilic attack toward the C-4 atom by HSO_3^- . These results show that DPS can readily react with bisulfite through specific nucleophilic addition reaction. Such reaction can be employed for the detection of HSO_3^- with high specificity.

The result shows that DPS can readily react with bisulfite through specific nucleophilic addition reaction. Such reaction can be employed for the detection of HSO_3^- with high specificity. We then try to combine the fluorescence quenching of DPS and

the stable fluorescence of graphene oxide to design a ratiometric method for bisulfite. Ratiometric method can enhance signal sensitivity and eliminate ambiguities by interference from environmental or instrumental efficiency. Thus we introduced fluorescent Hex-FGO as supporting material to transform a single fluorescence quenching signal to ratiometric fluorescence signal. The fluorescent Hex-FGO consists of two types of groups at the lateral edge and basal surface of GO nanosheets, such as alkylamides and 1, 2-amino alcohols, respectively. The surface functional groups can be supported by FT-IR spectra (Fig. S11). We can see that the carboxylic group bands at 1732 and 1250 cm^{-1} of original GO becomes weak after the treatment with hexamethylenediamine, while a new band near 1668 cm^{-1} appears which can be assigned to the C=O stretching of amide bond [44]. The emerging band at 1460 cm^{-1} should be assigned to the stretching vibration of $-\text{CONH}-$ [45]. The C=C vibration of aromatic rings with characteristic band at 1623 cm^{-1} appear in both Hex-FGO and original GO samples, showing that the typical sp^2 hybrid withheld after the modification process. The results suggest the covalent modification of hexamethylenediamine on the surface of GO through the amide reaction.

The excitation or absorption spectrum of DPS is partially overlapped with the emission spectrum of Hex-FGO (Fig. S12) and there is a fluorescence resonance energy transfer (FRET) from Hex-FGO to DPS, hence the system shows a bright yellow fluorescence from DPS when excited under 370 nm. Bisulfite can rapidly react with DPS and break the conjugated system, which results in the blue-shift of the product's absorption and reduce the FRET efficiency from Hex-FGO to the product. This process restores the fluorescence of Hex-FGO. Based on the above principle, we thus assemble the fluorescent Hex-FGO and DPS to construct a ratiometric fluorescent nanocomposite probe for sensing sulfur dioxide, which can produce fluorescence ratiometric variation. The nanocomposite exhibited a unique signal response when compared with the DPS compound alone. As shown in Fig. 1, the fluorescence intensity of the DPS gradually decreased nearly 9.6 folds upon the addition of HSO_3^- in a “turn off” manner. However, the nanocomposite of Hex-FGO-DPS has a maximum emission wavelength at 580 nm and

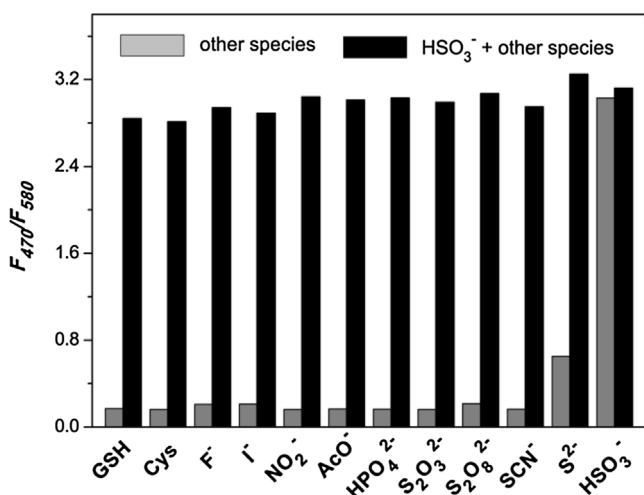


Fig. 3. The selectivity of the Hex-FGO-DPS (5 μM) system toward various anions and mercaptoamino-acid. Gray bars represent the addition of 100 μM each other species (25 μM of HSO_3^-) to a 5 μM solution of Hex-FGO-DPS, black bars represent the subsequent addition of 35 μM HSO_3^- to the solution. Excitation was provided at 370 nm.

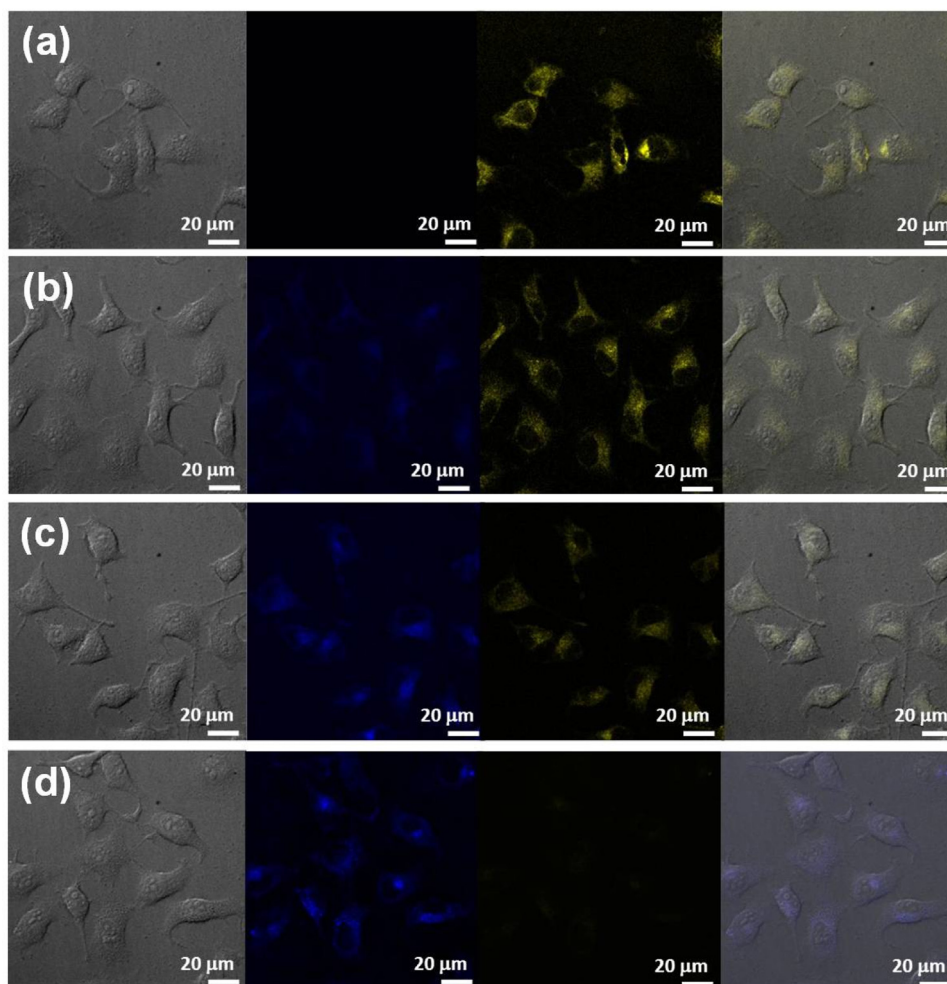


Fig. 4. Confocal fluorescence imaging of (a) living MCF-7 cells incubated with 10 μM Hex-FGO-DPS for 30 min; (b)–(d) MCF-7 cells loading with 10 μM Hex-FGO-DPS and further incubated with 25 μM , 50 μM , 75 μM of HSO_3^- for another 30 min, respectively. The four imaging columns represent the bright-field, blue channel, yellow channel, and the ratio overlay images (left to right). Excitation at 405 nm for collect image from the blue channel (460–480 nm) and yellow channel (560–580 nm). (For interpretation of the references to colour in this figure legend, the reader is referred to the web version of this article.)

a feeble emission wavelength at 470 nm. When exposed to HSO_3^- , the emission intensity at 580 nm decreased due to the block of FRET process, accompanied by the emission intensity at 470 nm enhanced. The ratiometric fluorescence intensity of Hex-FGO-DPS ($F_{470\text{nm}}/F_{580\text{nm}}$) changed near upon 25 folds. Clearly, the nanocomposite probe possesses two advantages. First, the Hex-FGO-DPS presents dramatically fluorescence variation which is dependent on the addition amount of HSO_3^- . Second, more detailed comparison could be made with a distinct color change from yellow to blue which demonstrate that the ratiometric probe is more easily visualized in a large color variation range than a single color regression change of individual DPS.

The dose-responsive manner of the Hex-FGO-DPS to HSO_3^- has been examined. Before addition of HSO_3^- , the ratiometric probe emits a distinct emission band centered at 580 nm (excitation wavelength 370 nm), which can be ascribed to the fluorescence of DPS. The emission band assigning to Hex-FGO seems very faint. When exposed to HSO_3^- , the fluorescence intensity at 580 nm of DPS decreased greatly and the fluorescence intensity at 470 nm of Hex-FGO increased (Fig. 2A). Meanwhile, the fluorescence color of the probe solution constantly evolved from yellow to green and then blue, due to the variation in the intensity ratio of the two emission wavelengths (Fig. 2A, below). Therefore, the sensitive color change shows the feasibility of the Hex-FGO-DPS probe for

visual detection of HSO_3^- under a UV lamp. Fig. 2B showed the plot of ratiometric fluorescence change against the concentration of HSO_3^- ranging from 5×10^{-6} to 2.5×10^{-5} M, which can be used for the quantification of HSO_3^- with a correlation coefficient of 0.9946. The limit of detection (LOD) was found to be 0.44 μM which was comparative with most reported bisulfite probes in phosphate buffer (pH 7.0) based on the definition of three times the deviation of the blank signal (3σ).

In consideration of the comprehensive application of HSO_3^- , the effect of other bio-related anion and amino acid on ratiometric fluorescence intensity of Hex-FGO-DPS was investigated for their potential existence in cellular environment. The results show that other species including various anions and mercaptoamino-acid showed little effect on the intensity ratio of the fluorescence of the probe, as shown in Fig. 3. The sulfide solution can slightly enhance the ratiometric fluorescence intensity, but the quenching effect shows negligible variation as compared to that of HSO_3^- . In addition, the concentrations of the interfering anions and mercaptoamino-acid are at least 3 times higher than that of HSO_3^- , no apparent interference was observed in fluorescence intensity of the probe solution. The results indicate that the Hex-FGO-DPS has specific selectivity to HSO_3^- and anti-interference ability towards the coexistence of other species.

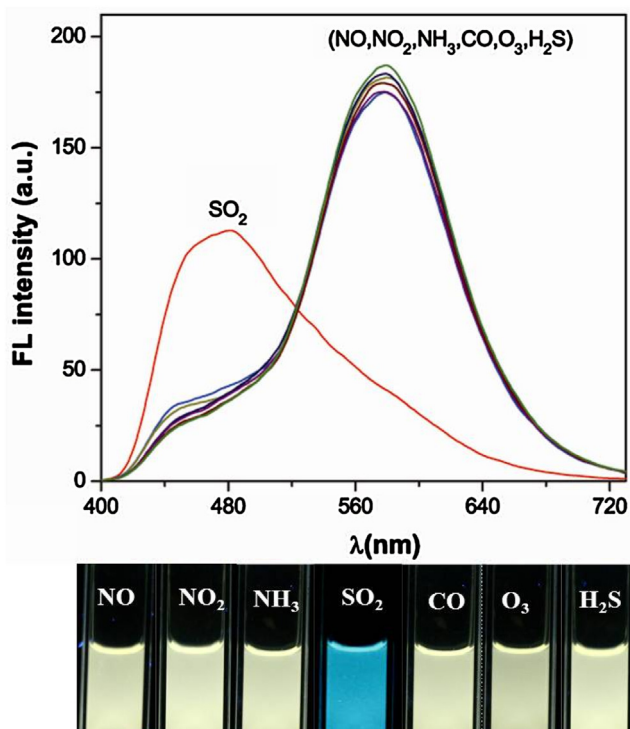


Fig. 5. Ratiometric fluorescent response of 5 μM Hex-FGO-DPS towards various gas species. Below: Color responses of Hex-FGO-DPS to different gas species under UV lamp with excitation at 365 nm in phosphate buffer 7.0 solution. The final concentration of SO_2 was 300 ppm; NO, NO_2 , NH_3 , CO, O_3 and H_2S were 1×10^3 ppm, respectively.

The potential application of the Hex-FGO-DPS for monitoring the variation of HSO_3^- level in living cells has been investigated by confocal fluorescence imaging. First, the cytotoxicity of the nanocomposite to MCF-7 cells was determined by an MTT assay with the concentrations of probe ranging from 0 to 20 μM (Fig. S13). Clearly, nearly 100% cell viability remained after incubation with 20 μM of the nanocomposite for 24 h, suggesting that probe is almost nontoxic for MCF-7 cells. Then, Hex-FGO-DPS with fixed concentration was introduced to the MCF-7 cell medium and incubated for 30 min. Under excitation at 405 nm, the ratio images of cell medium was collected from two channels (blue channel: 460–480 nm, yellow channel: 560–580 nm). As shown in Fig. 4a, a bright yellow fluorescence signals in the yellow channel were gathered, which indicated that Hex-FGO-DPS had remarkable membrane permeability. However, nearly no intracellular fluorescence signals in the blue channel were collected, suggesting that the intracellular presence of FRET process still exist. When bisulfite was introduced, the yellow fluorescence intensity gradually becomes darkening and eventually disappears, accompanied by brightening of blue fluorescence channel. The results indicate that Hex-FGO-DPS work well for sensing intracellular HSO_3^- changes through the ratiometric fluorescence imaging in living cells.

It is well known that sulfur dioxide can easily transfer to its derivatives bisulfite (HSO_3^-) and sulfite (SO_3^{2-}) (3:1 M/M, in neutral solution), we then discussed the ratiometric fluorescence response of Hex-FGO-DPS toward gaseous SO_2 in air. The fluorescence intensity of Hex-FGO-DPS at 580 nm and 470 nm were gradually changed through a meristic manner with the increased amount of gaseous SO_2 from 0 to 350 ppm, as shown in Fig. S14. The signal responses to gaseous sulfur dioxide is nearly identical with that of HSO_3^- , showing that Hex-FGO-DPS is also a powerful tool for the determination of gaseous SO_2 in aqueous solution. Then we evaluated the selectivity of Hex-FGO-DPS for identifying

gaseous SO_2 from other common gases, including NO, NO_2 , NH_3 , CO, O_3 and H_2S at higher concentrations. The results showed that these gases had no apparent spectral changes to the probe solution, as illustrated in Fig. 5 variation. Accordingly, the fluorescence color of the probe solution kept yellow after adding other gas species except that adding SO_2 turned blue. These results suggested that Hex-FGO-DPS can be also used for visual detection of gaseous SO_2 efficiently in complicated atmospheric samples.

4. Conclusion

In summary, we synthesized and prepared a new ratiometric probe combined with cyanine dye and fluorescent graphene oxide for sensitive detection of bisulfite and gaseous SO_2 . The as-prepared probe emits bright yellow fluorescence in aqueous solution and then distinctly changes to green and further blue with the addition amount of HSO_3^- . Therefore, the emission ratio of probe can be used to quantitative measuring of HSO_3^- and the limit of detection was calculated as 0.44 μM in aqueous solution. Importantly, when incubated the probe in MCF-7 cells, it exhibits multicolor images from yellow to blue in the presence of HSO_3^- . Moreover, the probe also operated well for gaseous SO_2 both in solution and air with noticeable spectral and fluorescence color variation. This designed method may open the possibility for simply, accurately and feasibly detecting of other gas molecules both in vitro and in vivo.

Acknowledgements

We acknowledge the financial support from the National Natural Science Foundation of China (Grant Nos. 21475134, 21507135, 91439101, 31571020, and 31300697) and the Fundamental Research Funds for the Central Universities (2016ZZD06), Anhui Provincial Natural Science Foundation of China (1608085MB30).

Appendix A. Supplementary data

Supplementary data associated with this article can be found, in the online version, at <http://dx.doi.org/10.1016/j.snb.2017.03.101>.

References

- [1] T.M. Chen, J. Gokhale, S. Shofer, W.G. Kuschner, Outdoor air pollution: nitrogen dioxide, sulfur dioxide, and carbon monoxide health effects, *Am. J. Med. Sci.* 333 (2007) 249–256.
- [2] D.Q. Rich, J. Schwartz, M.A. Mittleman, M. Link, H. Luttmann-Gibson, P.J. Catalano, F.E. Speizer, D.W. Dockery, Association of short-term ambient air pollution concentrations and ventricular arrhythmias, *Am. J. Epidemiol.* 161 (2005) 1123–1132.
- [3] M.H. Stipanuk, J.E. Dominy Jr., J. Lee, R.M. Coloso, Mammalian cysteine metabolism: new insights into regulation of cysteine metabolism, *J. Nutr.* 136 (2006) 1652S–1659S.
- [4] S. Iwasawa, Y. Kikuchi, Y. Nishiwaki, M. Nakano, T. Michikawa, T. Tsuboi, S. Tanaka, T. Uemura, A. Ishigami, H. Nakashima, Effects of SO_2 on respiratory system of adult Miyakejima resident 2 years after returning to the island, *J. Occup. Health* 51 (2009) 38–47.
- [5] X.J. Shi, Generation of SO_3^- and OH radicals in $\text{SO}_3(2^-)$ reactions with inorganic environmental pollutants and its implications to $\text{SO}_3(2^-)$ toxicity, *Inorg. Biochem.* 56 (1994) 155–165.
- [6] N. Sang, Y. Yun, H. Li, L. Hou, M. Han, G. Li, SO_2 inhalation contributes to the development and progression of ischemic stroke in the brain, *Toxicol. Sci.* 114 (2010) 226–236.
- [7] S. Faldt, B. Karlberg, W. Frenzel, Hyphenation of gas-diffusion separation and ion chromatography. Part 1: determination of free sulfite in wines, *Fresenius J. Anal. Chem.* 371 (2001) 425.
- [8] L. Pizzoferrato, G. Di Lullo, E. Quattrucci, Determination of free, bound and total sulphites in foods by indirect photometry-HPLC, *Food Chem.* 63 (1998) 275–279.
- [9] R.F. McFeeters, A.O. Barish, Sulfite analysis of fruits and vegetables by high-performance liquid chromatography (HPLC) with ultraviolet spectrophotometric detection, *J. Agric. Food Chem.* 51 (2003) 1513–1517.
- [10] U.T. Yilmaz, G. Somer, Determination of trace sulfite by direct and indirect methods using differential pulse polarography, *Anal. Chim. Acta* 603 (2007) 30–35.

- [11] D. Huang, B. Xu, J. Tang, J. Luo, L. Chen, L. Yang, Z. Yang, S. Bi, Indirect determination of sulfide ions in water samples at trace level by anodic stripping voltammetry using mercury film electrode, *Anal. Methods* 2 (2010) 154–158.
- [12] B. Palenzuela, B.M. Simonet, A. Rios, M. Valcarcel, Determination of free and total sulphur dioxide in wine by use of an amalgamated piezoelectric sensor, *Anal. Chim. Acta* 535 (2005) 65–72.
- [13] Z. Daunoravicius, A. Padarauskas, Capillary electrophoretic determination of thiosulfate, sulfide and sulfite using in-capillary derivatization with iodine, *Electrophoresis* 23 (2002) 2439–2444.
- [14] G. Jankovskiene, Z. Daunoravicius, A. Padarauskas, Capillary electrophoretic determination of sulfite using the zone-passing technique of in-capillary derivatization, *J. Chromatogr. A* 934 (2001) 67–73.
- [15] Y.Q. Sun, J. Liu, J.Y. Zhang, T. Yang, W. Guo, Fluorescent probe for biological gas SO₂ derivatives bisulfite and sulfite, *Chem. Commun.* 49 (2013) 2637–2639.
- [16] W. Xu, C.L. Teoh, J.J. Peng, D.D. Su, L. Yuan, Y.T. Chang, A mitochondria-targeted ratiometric fluorescent probe to monitor endogenously generated sulfur dioxide derivatives in living cells, *Biomaterials* 56 (2015) 1–9.
- [17] J.C. Xu, J. Pan, X.M. Jiang, C.Q. Qin, L.T. Zeng, H. Zhang, J.F. Zhang, A mitochondria-targeted ratiometric fluorescent probe for rapid, sensitive and specific detection of biological SO₂ derivatives in living cells, *Biosens. Bioelectron.* 77 (2016) 725–732.
- [18] W.Q. Chen, Q. Fang, D.L. Yang, H.Y. Zhang, X.Z. Song, J. Foley, Selective, highly sensitive fluorescent probe for the detection of sulfur dioxide derivatives in aqueous and biological environments, *Anal. Chem.* 87 (2015) 609–616.
- [19] Y. Liu, K. Li, M.Y. Wu, Y.H. Liu, Y.M. Xie, X.Q. Yu, A mitochondria-targeted colorimetric and ratiometric fluorescent probe for biological SO₂ derivatives in living cells, *Chem. Commun.* 51 (2015) 10236–10239.
- [20] Y. Liu, K. Li, K.X. Xie, L.L. Li, K.K. Yu, X. Wang, X.Q. Yu, A water-soluble and fast-response mitochondria-targeted fluorescent probe for colorimetric and ratiometric sensing of endogenously generated SO₂ derivatives in living cells, *Chem. Commun.* 52 (2016) 3430–3433.
- [21] Y.J. Zhang, L.M. Guan, H. Yu, Y.H. Yan, L.B. Du, Y. Liu, M.T. Sun, D.J. Huang, S.H. Wang, Reversible fluorescent probe for selective detection and cell imaging of oxidative stress indicator bisulfite, *Anal. Chem.* 88 (2016) 4426–4431.
- [22] M.T. Sun, H. Yu, K. Zhang, Y.J. Zhang, Y.H. Yan, D.J. Huang, S.H. Wang, Determination of gaseous sulfur dioxide and its derivatives via fluorescence enhancement based on cyanine dye functionalized carbon nanodots, *Anal. Chem.* 86 (2014) 9381–9385.
- [23] H.H. Li, H.J. Zhu, M.T. Sun, Y.H. Yan, K. Zhang, D.J. Huang, S.H. Wang, Manipulating the surface chemistry of quantum dots for sensitive ratiometric fluorescence detection of sulfur dioxide, *Langmuir* 31 (2015) 8667–8671.
- [24] X.F. Gu, C.H. Liu, Y.C. Zhu, Y.Z. Zhu, A boron-dipyrromethene-based fluorescent probe for colorimetric and ratiometric detection of sulfite, *J. Agric. Food Chem.* 59 (2011) 11935–11939.
- [25] M.G. Choi, J. Hwang, S. Eor, S.K. Chang, Chromogenic and fluorogenic signaling of sulfite by selective deprotection of resorufin levulinatate, *Org. Lett.* 12 (2010) 5624–5627.
- [26] G.Y. Li, Y. Chen, J.Q. Wang, J.H. Wu, G. Gasser, L.N. Ji, H. Chao, Direct imaging of biological sulfur dioxide derivatives in vivo using a two-photon phosphorescent probe, *Biomaterials* 63 (2015) 128–136.
- [27] G.Y. Li, Y. Chen, J.Q. Wang, Q. Lin, J. Zhao, L.N. Jia, H. Chao, UV-induced transformation of four halobenzoquinones in drinking water, *Chem. Sci.* 4 (2013) 4426–4433.
- [28] X.F. Yang, M. Zhao, G. Wang, A rhodamine-based fluorescent probe selective for bisulfite anion in aqueous ethanol media, *Sens. Actuators B* 152 (2011) 8–13.
- [29] X. Cheng, H. Jia, J. Feng, J. Qin, Z. Li, Reactive probe for hydrogen sulfite: turn-on fluorescent sensing and bioimaging application, *J. Mater. Chem. B* 1 (2013) 4110–4114.
- [30] Y. Yang, F. Huo, J. Zhang, Z. Xie, J. Chao, C. Yin, H. Tong, D. Liu, S. Jin, F. Cheng, X. Yan, A novel coumarin-based fluorescent probe for selective detection of bisulfite anions in water and sugar samples, *Sens. Actuators B* 166–167 (2012) 665–670.
- [31] X. Cheng, H. Jia, J. Feng, J. Qin, Z. Li, Reactive probe for hydrogen sulfite: good ratiometric response and bioimaging application, *Sens. Actuators B* 184 (2013) 274–280.
- [32] G. Eda, Y.Y. Lin, C. Mattevi, H. Yamaguchi, H.A. Chen, I.S. Chen, C.W. Chen, M. Chhowalla, Blue photoluminescence from chemically derived graphene oxide, *Adv. Mater.* 22 (2010) 505–509.
- [33] Q.S. Mei, K. Zhang, G.J. Guan, B.H. Liu, S.H. Wang, Z.P. Zhang, Highly efficient photoluminescent graphene oxide with tunable surface properties, *Chem. Commun.* 46 (2010) 7319–7321.
- [34] Z. Zhang, S. Achilefu, Synthesis and evaluation of polyhydroxylated near-infrared carbocyanine molecular probes, *Org. Lett.* 6 (2004) 2067–2070.
- [35] D.Y. Pan, J.C. Zhang, Z. Li, M.H. Wu, Hydrothermal route for cutting graphene sheets into blue-luminescent graphene quantum dots, *Adv. Mater.* 22 (2010) 734–738.
- [36] H.J. Zhu, W. Zhang, K. Zhang, S.H. Wang, Dual-emission of a fluorescent graphene oxide–quantum dot nanohybrid for sensitive and selective visual sensor applications based on ratiometric fluorescence, *Nanotechnology* 23 (2012) 315502.
- [37] Q.S. Mei, Z.P. Zhang, Photoluminescent graphene oxide ink to print sensors onto microporous membranes for versatile visualization bioassays, *Angew. Chem. Int. Ed.* 51 (2012) 5602–5606.
- [38] J. Geng, H. Jung, Porphyrin functionalized graphene sheets in aqueous suspensions: from the preparation of graphene sheets to highly conductive graphene films, *J. Phys. Chem. C* 114 (2010) 8227–8234.
- [39] K.P. Loh, Q.L. Bao, P.K. Ang, J.X. Yang, The chemistry of grapheme, *J. Mater. Chem.* 20 (2010) 2277–2289.
- [40] H.J. Zhu, Y.J. Zhang, L.L. Zhang, T. Yu, K. Zhang, H. Jiang, L.J. Wu, S.H. Wang, Highly photostable and biocompatible graphene oxides with amino acid functionalities, *J. Mater. Chem. C* 2 (2014) 7126–7132.
- [41] Z. Lou, P. Li, K. Han, Redox-responsive fluorescent probes with different design strategies, *Acc. Chem. Res.* 48 (2015) 1358–1368.
- [42] F. Yu, P. Li, B. Wang, K. Han, Reversible near-infrared fluorescent probe introducing tellurium to mimetic glutathione peroxidase for monitoring the redox cycles between peroxynitrite and glutathione in vivo, *J. Am. Chem. Soc.* 135 (2013) 7674–7680.
- [43] F. Yu, P. Li, G. Li, G. Zhao, T. Chu, K. Han, A near-IR reversible fluorescent probe modulated by selenium for monitoring peroxynitrite and imaging in living cells, *J. Am. Chem. Soc.* 133 (2011) 11030–11033.
- [44] O.C. Compton, D.A. Dikin, K.W. Putz, L.C. Brinson, S.T. Nguyen, Electrically conductive alkylated graphene paper via chemical reduction of amine-functionalized graphene oxide paper, *Adv. Mater.* 22 (2010) 892–896.
- [45] M. Aydin, Z. Kartal, S. Osmanoglu, M.H. Baskan, R. Topkaya, EPR and FT-IR spectroscopic studies of l-lysine monohydrochloride and l-glutamic acid hydrochloride powders, *J. Mol. Struct.* 994 (2011) 150–154.

Biographies

Huan Yu received her master degree (2012) in analytical chemistry from state key laboratory of chemo/biosensing and chemometrics, Hunan University. Presently, she is a research assistant at the Institute of Intelligent Machines, Chinese Academy of Sciences. Her current research mainly focused on the design and synthesis of fluorescent probes for detection of environmental pollutants and bioactive molecules.

Libo Du is currently an associate professor at State Key Laboratory for Structural Chemistry of Unstable and Stable Species, Institute of Chemistry, Chinese Academy of Sciences. His PhD research was performed at the Institute of Chemistry, Chinese Academy of Sciences. His research interests includes as follows: design, synthesis and application of fluorescent probes; design and synthesis of nanomaterials; fundamental understanding of biological effects of nanomaterials and their application.

Lingmei Guan received her master degree in 2016 from the Institute of Chemistry, Chinese Academy of Sciences. Her research interests mainly focused on the design and synthesis of fluorescent probes for detection of reactive oxygen species.

Kui Zhang is an associate professor at the Institute of Intelligent Machines, Chinese Academy of Sciences. He got a PhD from University of Science and Technology of China in 2011. His current research interests include optical functional materials, optical detection technology for pesticide in the environment.

Yingyun Li received his bachelor degree in 2014 from University of Jinan. He is currently a master's graduate student at Department of Materials Science and Engineering, University of Science and Technology of China. His research interests focus on the design and synthesis of organic fluorescent molecules for environmental pollutants detection.

Houjuan Zhu received her Ph.D. degree at the Institute of Intelligent Machines, Chinese Academy of Sciences. Her current research interests are focused on the design and synthesis of fluorescent nanomaterials for detection of environmental pollutants.

Mingtai Sun conducted his doctor studies in organic chemistry at Jilin University. He is currently an associate Professor at Institute of Intelligent Machines, Chinese Academy of Sciences. His research is focused on the design and synthesis of organic fluorescent molecules for biological reactive oxygen species detection.

Suhua Wang is a professor at the School of Environment and Chemical Engineering, North China Electric Power University. He got a PhD from Hong Kong University of Science and Technology. His current research interests focus on functional materials, analytical chemistry, and detection of hazardous substances in environment.